Proc. Natl. Acad. Sci. USA
Vol. 91, pp. 3530–3533, April 1994
Developmental Biology

Magnetic resonance microscopy of mouse embryos

(embryonic anatomy/three-dimensional imaging/bovine serum albumin-diethylenetriaminepentaacetic anhydride-gadolinium/contrast agent)

BRADLEY R. SMITH*, G. ALLAN JOHNSON*, ERNEST V. GROMAN†, AND ELWOOD LINNEY‡§

*Department of Radiology, Box 3302, and ‡Department of Microbiology, Box 3020, Duke University Medical Center, Durham, NC 27710; and †Advanced Magnetics, 61 Mooney Street, Cambridge, MA 02138

Communicated by D. Bernard Amos, January 3, 1994 (received for review October 20, 1993)

ABSTRACT **The increased use of the mouse as a model for various aspects of mammalian biology has caused a renewed interest in developing strategies for examining and comparing normal and abnormal mouse embryonic development and anatomy. In this study, we have explored the use of magnetic resonance microscopy as a tool for these purposes. Techniques for the fixation, embedding, perfusion, and image acquisition of mouse embryos are described. The perfusion of bovine serum albumin-diethylenetriaminepentaacetic anhydride-gadolinium as a contrast agent enhances images of the developing embryonic vasculature during critical stages of organogenesis and allows for comparisons when embryos have been treated with teratogens such as retinoic acid. The acquired three-dimensional data sets are available for archiving, distributing, and postacquisition manipulations such as computer segmentation of anatomical structures.**

The mouse has become the animal model of choice for studying mammalian embryonic development because of the experimental techniques that have developed around it and because of its long and detailed history as a genetic model. However, technologies for analysis of developmental anatomy and mutant structures have not kept pace with technologies involving the manipulation of the mouse germ line to produce these developmental phenotypes. The storage, interpretation, and dissemination of the large amounts of data on these abnormal phenotypes presents an important challenge. The wide acceptance of the mouse as a preferred animal model is complemented by the extensive collection and documentation of >1000 mutant loci of mice (1). Transgenic technology has become commonplace, allowing the transfer of foreign genes into the mouse germ line and has led to the growth of service laboratories producing many lines of transgenic mice for investigators. Additionally, the germ line of mice can be manipulated by targeting mutations into specific genes in embryonic stem cells, making it possible to study the immediate and ultimate functions of the specific genes (2). A vast body of *in situ* hybridization information concerning the three-dimensional expression patterns of genes in the mouse embryo is quickly developing as more genes are isolated and examined. Current formats for describing morphological abnormalities of embryonic gene expression are inadequate because they are two dimensional, whereas the information being generated is three and four dimensional. In addition, investigators creating abnormal mice do not always have adequate training to evaluate the morphological changes being studied. For these reasons, there is a growing need for a means by which multidimensional anatomy can be recorded and easily transmitted to many investigators.

The publication costs of this article were defrayed in part by page charge payment. This article must therefore be hereby marked "*advertisement*" in accordance with 18 U.S.C. §1734 solely to indicate this fact.

In this report, we describe how magnetic resonance (MR) microscopy can be used to acquire three-dimensional data sets of embryonic anatomy for study on personal computers, how the embryonic vasculature can be enhanced and examined, and how anatomical structures can be computer-segmented from acquired three-dimensional data sets. To enhance the imaging of the vasculature, we use a macromolecular contrast agent: bovine serum albumin coupled to the chelating agent diethylenetriaminepentaacetic anhydride (DTPA) followed by interaction of this macromolecular complex with gadolinium chloride (Gd) (BSA-DTPA-Gd) (3–5). While we present two-dimensional images of the vasculature in this report, it should be pointed out that they are derived from three-dimensional data sets that allow the subject to be viewed from any orientation. The data sets are suitable for archiving, annotating, and distributing as three-dimensional records of each mouse developmental stage and are accessible to common personal computers such as PCs and Macintoshes.

METHODS

Animals are maintained according to protocols approved by the Institutional Animal Care and Use Committee and Public Health Service guidelines. Embryos are surgically extracted from the anesthetized female [2.5% (vol/vol) Avertin, 0.015 ml/g of body weight]. Phosphate-buffered saline is perfused into the umbilical vein of the mouse embryo followed by a fixative perfusion [2% (vol/vol) glutaraldehyde/1% formalin in phosphate buffer at 300 milliosmoles/liter] and finally the contrast agent, BSA-DTPA-Gd with ≈1 mM Gd, dissolved in a 10% (wt/vol) gelatin solution is perfused through the umbilical artery (20). After the perfusions, the embryos are quickly immersed in phosphate-buffered saline at 4°C to solidify the gelatin and then immersion-fixed until they are embedded in 3% low-melting-point agarose for MR microscopy analysis. All data are acquired at 9.4 T by using a GE NMR Instruments Omega system modified for MR microscopy. A 1-cm-solenoid radio-frequency coil has been constructed from a single sheet of dielectric microwave substrate. Data are acquired using three-dimensional spin warp encoding adapted for imaging of large arrays (currently up to 512^3) with repetition in pulse sequence (TR) = 200 ms, echo time (TE) = 6 ms, and four excitations for each phase-encoding step. Scanning data are reconstructed by Fourier transform on a Sparc 1 workstation (Sun Microsystems, Mountain View, CA). The resulting 256 16-bit image slices are archived and then scaled to 8 bits for volume rendering on a Silicon Graphics workstation (Iris 4D/320VGX, Silicon Graphics, Mountain View, CA) using VOXELVIEW_ULTRA 2.0 (Vital Images, Fairfield, IA). This program supports volume

Abbreviations: MR, magnetic resonance; BSA, bovine serum albumin; DTPA, diethylenetriaminepentaacetic anhydride; Gd, gadolinium chloride.

§To whom reprint requests should be addressed.

rendering using ray tracing (6–8). Final volume-rendered images, such as those presented in this report, are annotated and composited on Macintosh computers and out-put to film on a 35-mm film recorder.

RESULTS

MR microscopy provides the ability to document and disseminate the type of multidimensional data from developmental anatomy that is being generated by numerous laboratories. It is a nondestructive and distortion-free technique suited for studying and documenting both normal and abnormal morphogenesis of embryos during important time periods of development. MR microscopy is similar in some sense to magnetic resonance imaging (MRI) used in clinical practice. However, to achieve higher spatial resolution, MR microscopy differs from its clinical counterpart in two fundamental respects: much stronger encoding gradients are used and, to improve the sensitivity, a much higher magnetic field is required. Spatial encoding of the NMR response to a radio-frequency pulse is accomplished with magnetic field gradients. A major consequence of the strong encoding gradients in MR microscopy is that diffusion becomes an important determinant in the contrast in any image (9–11). The signal available from a tissue voxel (volumetric pixel) is dependent on the volume of the voxel. The volume of a voxel in MR microscopy is as much as a million times smaller than one in conventional MRI. The high magnetic fields used in MR microscopy also has major consequences for the contrast in the images because many of the parameters (T1, T2, etc.) are field-dependent (12, 13). MR microscopy differs from optical microscopy in two major ways: it is inherently three dimensional and contrast in the image is dependent on the nature of the bound water in the specimen. The tissue is interrogated using radio-frequency pulses. The tissue is transparent to these pulses so there is no need to physically section the specimen. Thus valuable specimens can be studied with safety. Moreover, the same specimen can be imaged many times using any of a number of different contrast mechanisms. Since MR exploits the proton resonance, the image can emphasize any of a variety of mechanisms that tell us something about water and how it is bound in the tissue. In the studies shown here, contrast in the images is determined by differences in proton density and T1. But there are many other contrast mechanisms available. Our imaging scheme acquires three-dimensional data sets of isotropic voxels (volumetric pixel units with equal dimensions in all three axes). This allows retrospective slicing of the specimen in any axis and at any thickness to be accomplished electronically (Fig. 1*a*). At embryonic day 16.5, distinct enhancement of skeletal structures is observed (see Fig. 1*b*). When enhancement of anatomical structures occurs that results in contiguous voxels sharing a signal intensity range, one can segment those structures from the rest of the data set using the VOXELVIEW

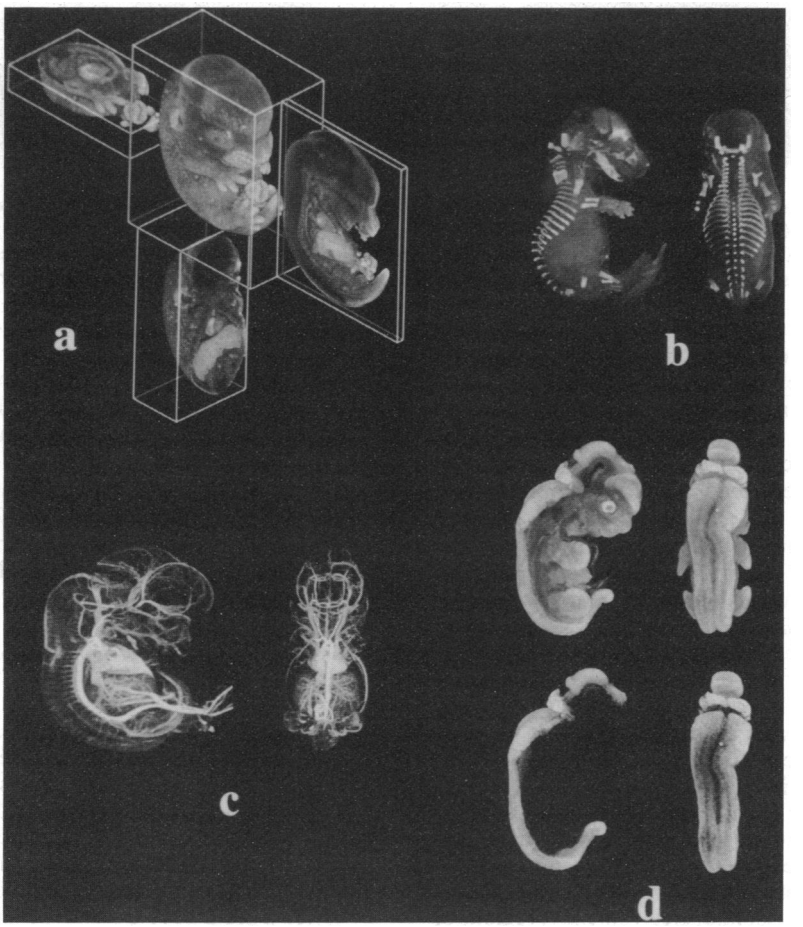

FIG. 1. (*a*) These volume-rendered images demonstrate the ability afforded by MR microscopy retrospectively to select planes of sectioning and the thickness of the sections to be viewed. The thicker slab renderings provide a "pseudo" confocal microscopic image of this day 14.5 mouse embryo (day 0.5 is defined as noon of the day a fertilization plug is found after overnight mating). (*b*) Volume-rendered MR scan of a day 16.5 mouse embryo, demonstrating the inherent contrast of the developing bones. (*c*) A day 12.5 mouse embryo was injected with BSA-DTPA-Gd in 10% gelatin and scanned by MR microscopy to obtain these maximum voxel renderings of the three-dimensional data set. (*d*) The completely open neural tube in a day 12.5 loop–tail mutant mouse embryo (14) is electronically segmented based on its contrast with surrounding tissues.

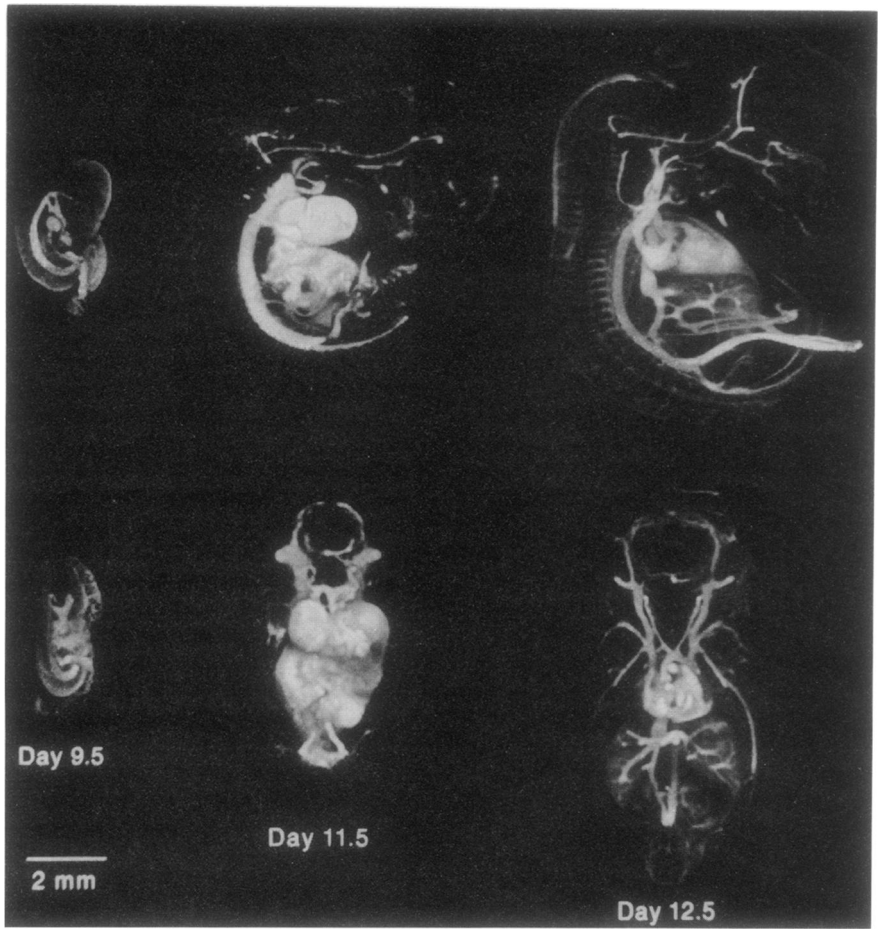

FIG. 2. Sagittal and coronal views of day 9.5, 11.5, and 12.5 mouse embryos are compared in these volume-rendered slabs generated by MR microscopy with BSA-DTPA-Gd used as a vascular contrast agent. The dorsal aorta and its segmental arteries dominate the sagittal views (upper row), although vessels as small as the third and fourth aortic arches are easily identified in the day 9.5 embryo. The pulmonary trunk (projecting out of the image plane) and ascending aortic arch are readily observed in the coronal view of the day 12.5 embryo (lower row).

program. Fig. 1*d* demonstrates the ability to use computer segmentation to isolate the neural tube of a mutant mouse embryo based on the inherent contrast between the neural tube tissues and surrounding tissues. This contrast is due to differences in the water binding characteristics of these tissues. Where inherent contrast is insufficient, extrinsic contrast agents can be used to enhance the signal in structures of interest (Fig. 1*c*).

Fig. 1*c* is a maximum intensity projection rendering of a three-dimensional data set from a day 12.5 mouse embryo. The completeness of vascular filling and the high signal intensity delivered by the BSA-DTPA-Gd contrast to vascular structures are clearly demonstrated here. Vessels from 50 μm (internal carotid artery and dorsal segmental arteries) to 200 μm (anterior cardinal vein) are readily identified.

The data in Fig. 2 are volume-rendered images of slabs containing the central one-third of each embryo's volume from sagittal and coronal views of day 9.5, day 11.5, and day 12.5 mouse embryos. The lateral two-thirds of data in the sagittal views and the anterior/posterior two-thirds in the coronal views were excluded to emphasize the central arterial structures. The venous anatomy otherwise obscures the arterial detail. This ability to isolate, electronically, regions of interest is another advantage afforded by MR microscopy.

In addition to comparing the three-dimensional anatomy of differing stages of mouse development, MR microscopy also allows for detailed comparisons of three-dimensional anatomy between normal and abnormal development. Fig. 3 compares the vasculature of a normal day 12.5 embryo with an abnormal mouse embryo at a similar age that had been exposed to the teratogen retinoic acid at day 9.5 (55 mg/kg). The contrast injection clearly permits the identification of abnormal vascular development in caudal structures of the embryo exposed to retinoic acid. The tail and hind limbs of the normal embryo are clearly vascularized while the absence of vascularization in the tail and right lower limb of the abnormal embryo punctuates the retinoic acid-induced hypoplasia of these structures (15). This vasculature imaging provides a "skeletal" structure by which abnormal morphology can be easily examined, since the vasculature follows the abnormal anatomy.

DISCUSSION

In this report we have emphasized the use of MR microscopy for studying a specific topic, normal and abnormal development of the embryonic vasculature. However, we have also completed the scanning and reconstruction of normal mouse embryos between days 9.5 and 18.5 of gestation. Our goal is to develop an archive based on three-dimensional data of the mouse from gestational day 8 to neonate and to make the archive addressable by personal computers.

While BSA-DTPA-Gd and Gd-dextran have been used to examine the vasculature of living organisms (3, 16–18), the use of gelatin with this contrast perfusion allows for greater image contrast and reproducibility due to the increased retention of the contrast agent. With vascular perfusion of BSA-DTPA-Gd followed by MR microscopic examination, we have been able to resolve and identify blood vessels down to 20 μm in diameter in mouse embryos at 9.5 days of

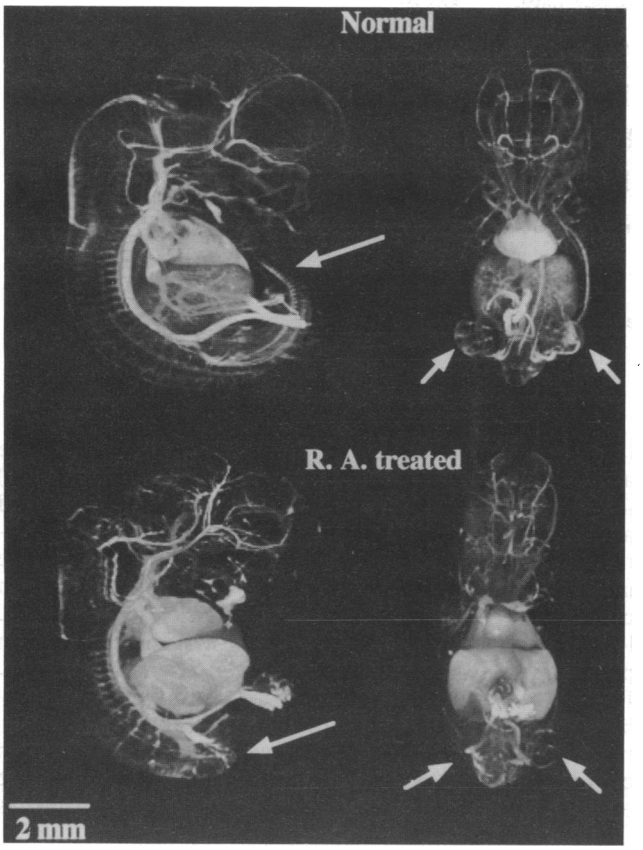

FIG. 3. Ability of MR microscopy with BSA-DTPA-Gd contrast enhancement to reveal distinctions between the vasculature in normal and abnormal mouse embryos. In the upper row, images are volume renderings of a normal day 12.5 mouse embryo, and in the lower row, images are from an embryo fed 55 mg of retinoic acid (R.A.) per kg of mouse weight at day 9.5 and imaged 3.5 days later. The retinoic acid-induced malformations include hypoplasia of the hind limbs and tail and are reflected in the concurrent hypoplasia of the vasculature in these regions (see arrows).

gestation. We are able to identify vascular malformations induced in the embryo by retinoic acid. These findings demonstrate the ability of MR microscopy to locate, identify, and document vascular morphogenesis and dysmorphogenesis when combined with contrast enhancement. However, MR microscopy has limits with regard to resolution. They arise in two broad categories—those imposed by the fundamental physics and those imposed by the existing technologies. The major limits imposed in this work arise from the existing technology; the ability to rapidly acquire and reconstruct the large data arrays. Reconstruction and scaling eventually reduce the data arrays to sizes manageable to personal computers and the Macintosh, but the initial acquisition requires large and fast storage devices. Another resolution barrier is posed by the decreasing signal available from each voxel as those voxels are made smaller and smaller. Recent development of more sensitive probes promises to push this barrier to <10 μm (19). However, the nondestructive nature of MR microscopy, combined with the visualization techniques available for studying its isotropic data, make it an important tool for interrogating, documenting, and communicating developmental anatomy.

Some of the greatest benefits from MR microscopy for developmental anatomy should come from techniques that are still maturing. Imaging of live embryos should allow longitudinal studies of normal and abnormal development. This can be accomplished with *in utero* and embryo culture techniques. Mapping the three-dimensional and four-dimensional expression of genes will depend on our ability to directly or indirectly tag antibodies or antisense nucleic acid probes with MR contrast agents and then introduce these into the embryo at sufficient concentration to affect the MR signal. These techniques in combination with the design of contrast agent binding reporter transgenes hold great promise in elucidating many developmental processes.

We thank G. Cofer and S. Suddarth for support in MR microscopy acquisitions and reconstructions and M. Colbert and R. Kelsey for aid with the embryo preparations. We are grateful to J. Knoplioch and G. Prevost of General Electric Medical Systems, Europe, for providing us a β release of VOXTOOL. This research was supported through a grant from the North Carolina Biotechnology Center, 9210-IDG-1016 (E.L.), and grants from the National Institutes of Health [RO1 HD24130, HD28855, and CA39066 (E.L.); P41 RR05959-01 (G.A.J.); RO2 ES04187-04A1 (G.A.J.)] and the National Science Foundation [CDR-8622201 (Engineering Resource Center)].

1. Lyon, M. F. & Searle, A. G. (1989) *Genetic Variants and Strains of the Laboratory Mouse* (Oxford Univ. Press, Oxford).
2. Capecchi, M. R. (1989) *Science* **244**, 1288–1292.
3. Ogan, M. D., Schmiedl, U., Moseley, M. E., Grodd, W., Paajanen, H. & Brasch, R. C. (1987) *Invest. Radiol.* **22**, 665–671.
4. Niemi, P., Koskinen, S. & Reisto, T. (1991) *Invest. Radiol.* **26**, 674–680.
5. Hnatowich, D. J., Layne, W. W. & Childs, R. L. (1982) *J. Appl. Radiat. Isot.* **33**, 327–332.
6. Argiro, V. J. (1990) *Pixel* **1**, 35–39.
7. Frenkel, K. A. (1989) *Commun. ACM* **32**, 426–435.
8. England, N. (1990) *Volume Visualization '90 Proceedings* (ACM Computer Graphics, San Diego).
9. Callaghan, P. T. & Eccles, C. D. (1988) *J. Magn. Reson.* **78**, 1–8.
10. Ahn, C. B. & Cho, Z. H. (1989) *Med. Phys.* **16**, 22–28.
11. Meyer, R. A. & Brown, T. R. (1988) *J. Magn. Reson.* **76**, 393–399.
12. Callaghan, P. T. (1991) *Nuclear Magnetic Resonance Microscopy* (Oxford, London).
13. Blümich, B. & Kuhn, W. (1992) *Magnetic Resonance Microscopy: Methods and Applications in Materials Science, Agriculture and Biomedicine* (VCH, Weinheim, F.R.G.).
14. Strong, L. C. & Hollander, W. F. (1949) *J. Hered.* **40**, 329–334.
15. Shenefelt, R. E. (1972) *Teratology* **5**, 103–118.
16. S.-c. Wang, Wikstrom, M. G., White, D. L., Klaveness, J., Holtz, E., Rongved, P., Moseley, M. E. & Brasch, R. C. (1990) *Radiology* **175**, 483–488.
17. Li, K. C. P., Quisling, R. G., Armitage, F. E., Richardson, D. & Christopher, M. (1992) *Magn. Reson. Imaging* **10**, 439–444.
18. Vexler, V. S., Berthezene, Y., Clement, O., Muhler, A., Rosenau, W., Moseley, M. E. & Brasch, R. C. (1992) *J. Magn. Reson. Imaging* **2**, 311–319.
19. Black, R. D., Early, T. A., Roemer, P. B., Mueller, O. M., Morgo-Campero, A., Turner, L. G. & Johnson, G. A. (1993) *Science* **259**, 793–795.
20. Effmann, E. L. (1982) *Invest. Radiol.* **17**, 529–538.